

Effect of Ancillary Ligands on the Proton-Transfer Reactivity of the Excited State of *trans*-Dioxorhenium(V)

Wentian Liu and H. Holden Thorp*

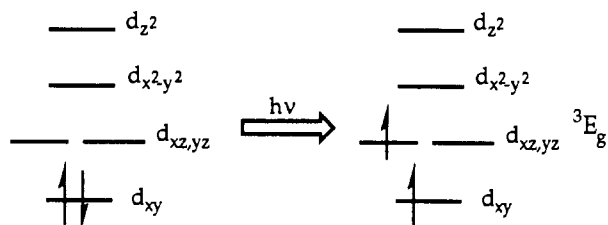
Department of Chemistry, The University of North Carolina, Chapel Hill, North Carolina 27599-3290

Received October 14, 1993*

Complexes based on *trans*-ReO₂⁺ exhibit long-lived emission from the ³E_g ligand-field excited state. This emission is quenched by proton transfer from a variety of acids. Reported here are results of emission quenching of ReO₂L₄⁺ (L = py, 3-Cl-py, 4-OMe-py) by common nitrogen and oxygen acids. Marcus analysis of the free energy dependence of the quenching rate constants points to a low barrier to proton transfer ($\lambda \sim 4$ kcal). The results of the analysis can be used to calculate a pK_a^{*} of 11.3 for the py complex, which is consistent with earlier results for metal hydride acids. For the py and 3-Cl-py complexes, the standard Marcus relation can be used; however, fitting of the data for the 4-OMe complex requires the introduction of an asymmetry parameter, ϵ , which is related to the degree of excited-state distortion in the chromophore. Comparison of the excited-state Re–O stretching frequency obtained from low-temperature absorption spectra with the corresponding ground-state frequency obtained from resonance Raman spectra shows that there is a larger excited-state distortion in the 4-OMe complex.

Transition-metal complexes exhibiting multiple bonding between the metal center and a coordinated ligand are of interest in a wide range of areas.^{1–5} Perhaps the simplest complexes that exhibit metal–ligand multiple bonding are metal–oxo complexes.^{4,5} Even though a large number of these complexes have been known for many years, several important issues involving the reactivity of these complexes remain unresolved. In particular, reactivity of metal–oxo complexes toward abstraction of hydrogen atoms from organic substrates is a consequence of coupling the redox chemistry of the metal center to the acid–base chemistry of the oxo ligand.^{5,6} This coupling has led to numerous useful catalysts and to unusual kinetic observations, such as large kinetic isotope effects.^{7,8} There is considerable understanding of the factors influencing the electron-transfer reactivity of metal centers, but the proton-transfer reactivity of the coordinated oxo ligand is poorly understood in comparison.

The emissive excited state of ReO₂(py)₄⁺ ($\lambda_{\text{max}}(\text{CH}_3\text{CN}) = 650$ nm, $\tau(\text{CH}_3\text{CN}) = 10$ μs) is created by promotion of an electron from the nonbonding d_{xy} orbital to the formally Re–O π -antibonding d_{xz,yz} level:⁹



Franck–Condon analysis of the vibronic structure seen in low-temperature absorption spectra of ReO₂⁺ demonstrates that the

Re–O bonds lengthen by 0.07 Å upon population of the ³E_g state, consistent with the addition of an electron to an antibonding orbital.⁹ The removal of an electron from a nonbonding metal-based orbital and addition of an electron to an antibonding metal–oxygen orbital imparts a degree of charge-transfer character to the transition, thus making the oxo ligand more electron rich (and, hence, more basic) in the excited state than in the ground state. In addition, the lengthening of the Re–O bond upon excitation creates an excited state that resembles the protonated form, which may dictate a low intrinsic barrier to protonation of the excited state.^{10–15}

We recently reported that the long-lived excited state of ReO₂(py)₄⁺ is readily protonated by a wide range of acids, and including typical oxygen and nitrogen acids¹⁶ as well as carbon acids and metal hydrides.¹⁷ In particular, we are interested in understanding the kinetics of the excited-state proton-transfer reaction as a function of thermodynamic driving force, kinetic acidity of the quencher, and the isotopes involved in the transfer reaction. We have reported that the kinetics of quenching of ReO₂(py)₄⁺ by common organic acids in acetonitrile solution follows a Rehm–Weller type dependence on free energy, with a parabolic region observed at low driving force that levels off at the diffusion-controlled limit.¹⁶ In addition to varying the pK_a of the acid quencher, one can also control the driving force of the reaction by adding substituents to the pyridine rings of the metal complex. We report here detailed studies on the quenching of ReO₂(py)₄⁺ and substituted derivatives by common organic acids over a wide range of thermodynamic acidities.

Experimental Section

The complexes [ReO₂(py)₄](PF₆), [ReO₂(4-OMe-py)₄](PF₆), and [ReO₂(3-Cl-py)₄](NO₃) were prepared by established procedures.^{18,19} Handling and preparation of quenchers were done as described previ-

* Abstract published in *Advance ACS Abstracts*, February 15, 1994.

- (1) Nugent, W. A.; Mayer, J. M. *Metal-Ligand Multiple Bonds*; Wiley: New York, 1988.
- (2) Paradis, J. A.; Wertz, D. W.; Thorp, H. H. *J. Am. Chem. Soc.* **1993**, *115*, 5308.
- (3) Sernette, A.; Carroll, P. J.; Swager, T. M. *J. Am. Chem. Soc.* **1992**, *114*, 1887. Pollagi, T. P.; Stoner, T. C.; Dallinger, R. F.; Gilbert, T. M.; Hopkins, M. D. *J. Am. Chem. Soc.* **1991**, *113*, 703.
- (4) Holm, R. H. *Chem. Rev.* **1987**, *87*, 1401.
- (5) Meyer, T. J. *J. Electrochem. Soc.* **1984**, *131*, 221C.
- (6) Thorp, H. H. *Chemtracts: Inorg. Chem.* **1991**, *3*, 171.
- (7) Cabaniss, G. E.; Diamantis, A. A.; Murphy, W. R., Jr.; Linton, R. W.; Meyer, T. J. *J. Am. Chem. Soc.* **1985**, *107*, 1845.
- (8) Binstead, R. A.; Meyer, T. J. *J. Am. Chem. Soc.* **1987**, *109*, 3287.
- (9) Winkler, J. R.; Gray, H. B. *Inorg. Chem.* **1985**, *24*, 346.

- (10) Thorp, H. H.; Kumar, C. V.; Turro, N. J.; Gray, H. B. *J. Am. Chem. Soc.* **1989**, *111*, 4364.
- (11) Newsham, M. D.; Giannelis, E. P.; Pinnavaia, T. J.; Nocera, D. G. *J. Am. Chem. Soc.* **1988**, *110*, 3885.
- (12) Thorp, H. H.; Gray, H. B. *Photochem. Photobiol.* **1991**, *54*, 609.
- (13) Thorp, H. H.; Turro, N. J.; Gray, H. B. *New J. Chem.* **1991**, *15*, 601.
- (14) Thorp, H. H.; Van Houten, J.; Gray, H. B. *Inorg. Chem.* **1989**, *28*, 889.
- (15) Brewer, J. C.; Thorp, H. H.; Brudvig, G. W.; Gray, H. B. *J. Am. Chem. Soc.* **1991**, *112*, 3171.
- (16) Liu, W.; Welch, T. W.; Thorp, H. H. *Inorg. Chem.* **1992**, *31*, 4044.
- (17) Goll, J. G.; Liu, W.; Thorp, H. H. *J. Am. Chem. Soc.* **1993**, *115*, 11048.
- (18) Brewer, J. C.; Gray, H. B. *Inorg. Chem.* **1989**, *28*, 3334.
- (19) Ram, M. S.; Hupp, J. T. *Inorg. Chem.* **1991**, *30*, 130.

ously.¹⁶ Quenching experiments were performed using a SPEX Fluoromax spectrophotometer fitted with a water-cooled sample holder for temperature-dependent quenching measurements, as described previously.^{16,20} Quenching rate constants were obtained from Stern–Volmer plots of emission intensity versus quencher concentration. At least five points and a correlation coefficient of >0.99 were obtained for each rate constant. We have shown previously that intensity and lifetime quenching give identical results in this system.^{9,16} Low-temperature absorption spectra were measured using quartz cells and a liquid nitrogen Dewar flask with quartz windows. Spectra were acquired using an OLIS-modified Cary 14. All fitting of data was performed using the Kaleidagraph software.

Raman spectra were measured using an ISA U1000 1.0-m scanning double monochromator operated under computer control using software provided by the manufacturer.²¹ The same software controlled data acquisition. Photon-counting detection using a thermoelectrically cooled Hamamatsu R943-02 photomultiplier tube was employed. Spectral slit width was set at 5 cm^{-1} . The Raman scattering was excited at 457.8 nm by a 5-W argon ion laser (Spectra-Physics Model 265). All samples were excited with about 50 mW of incident power, and Raman scattered light was collected at 135° from incidence. Samples were spun to minimize local heating and any photodegradation of the sample. UV–vis spectra measured before and after the Raman experiment were compared to ensure sample integrity throughout sample illumination.

Results and Discussion

The application of Marcus theory to ground-state proton-transfer reactions has been successful.^{22,23} In organic chemistry, proton-transfer kinetics are generally analyzed in terms of Bronsted plots of the logarithm of the proton-transfer rate constant versus the $\text{p}K_a$ of the acid donor; the slope of the plot gives the characteristic Bronsted α coefficient. The same rate constants can be also be analyzed using the Marcus equation

$$\Delta G^\ddagger = w^\ddagger + (\lambda/4)(1 + \Delta G/\lambda)^2 \quad (1)$$

where ΔG^\ddagger is the free energy of activation, w^\ddagger is the work required for solvent reorganization to form the encounter complex, ΔG is the actual free energy for the proton-transfer step itself, and $\lambda/4$ is the intrinsic barrier to reaction when $\Delta G = 0$. The Bronsted coefficient α for proton transfer is just $d\Delta G^\ddagger/d\Delta G$ or

$$\alpha = 1/2 + \Delta G/2\lambda \quad (2)$$

Thus, for Marcus theory to obtain, α must be 0.5 at $\Delta G = 0$, which will occur only if the potential energy surfaces of the product and reactant have nearly the same shape (Figure 1).^{23–25}

The extent of curvature of a Bronsted plot is then $d\alpha/d\Delta G$ or $1/2\lambda$. Slow reactions with large intrinsic barriers show essentially linear Bronsted plots, while fast reactions with small barriers should show distinct curvature.²⁴ Excited-state proton transfer in many organic systems is adequately described by eq 1. However, in many systems, such as styrenes, application of Marcus theory is complicated by the fact that the potential energy surfaces of organic excited states are much shallower than those of the corresponding ground states (Figure 1),^{24,25} leading to values for α that are significantly lower than 0.5. Using the Marcus equation in its usual form (eq 1) in these organic systems results in calculated values for λ and the $\text{p}K_a^*$ that are clearly unreasonable; however, it can be estimated using a modified Marcus equation that, for rapid ($10^7\text{ M}^{-1}\text{ s}^{-1}$) proton transfers to occur, the intrinsic barrier must be on the order of $\lambda/4 = 1\text{--}3\text{ kcal}$.²⁴

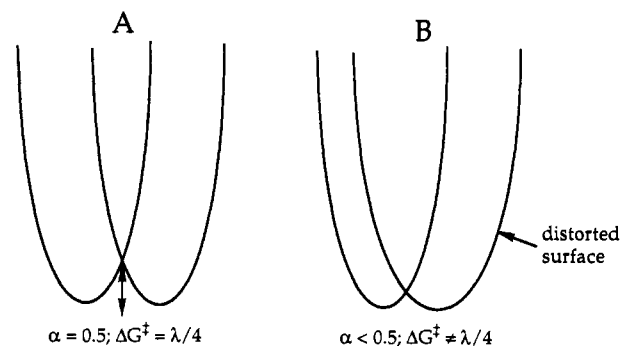


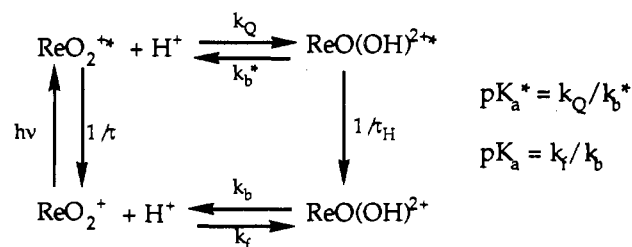
Figure 1. (A) Potential energy surfaces for a proton-transfer reaction that conforms to the unmodified Marcus equation. (B) Potential energy surfaces for a system where one partner of the reaction undergoes excited-state distortion.

Table 1. Excited- and Ground-State Proton-Transfer Parameters for ReO_2^+ Complexes

complex	ϵ^a	α - ($\Delta G=0$) ^a	gs $\text{p}K_a^b$	$\text{p}K_a^* \text{ }^{a,c}$	λ , kcal ^a
$\text{ReO}_2(3\text{-Cl-py})_4^+$	1	0.5	-0.5	11.0	4.2
$\text{ReO}_2(\text{py})_4^+$	1	0.5	-0.3	11.3	3.9
$\text{ReO}_2(4\text{-OMe-py})_4^+$	0.70–0.78	0.35	0.5	12.0–12.5	4–4.8

^a From fitting of free-energy dependence of quenching rate constants using eqs 3 and 8. ^b Reference 31. ^c On the aqueous scale.

Scheme 1



We have determined using the Stern–Volmer relation the quenching rate constants for reactions of the excited states of $\text{ReO}_2(\text{py})_4^+$, $\text{ReO}_2(3\text{-Cl-py})_4^+$, and $\text{ReO}_2(4\text{-OMe-py})_4^+$ with a family of common nitrogen and oxygen acids. Addition of electron-withdrawing and -releasing substituents to the pyridine ligand shifts the $\text{p}K_a$ of the ground state of the complex, as shown in Table 1. In the analysis of the quenching dynamics, the kinetic scheme in Scheme 1 is used. In order for the k_Q determined from Stern–Volmer quenching plots to give the true rate constant for reaction of ReO_2^{*+} with the acid quencher, the excited-state decay of the protonated form, $\text{ReO}(\text{OH})^{2+*}$, must be fast compared to deprotonation to form ReO_2^{*+} ; i.e., $1/\tau_{\text{H}} \gg k_b^*$. If this is the case, then the situation becomes completely analogous to excited-state electron transfer, where quenching of the excited state always leads to the *ground-state* oxidized or reduced forms. Other transition-metal systems usually exhibit emission from the protonated form, which complicates the kinetic analysis but allows for a straightforward determination of $\text{p}K_a^*$.^{26–29}

The assumption that $1/\tau_{\text{H}} \gg k_b^*$ is consistent with the observation that proton-transfer quenching of the emission intensity gives diffusion-controlled rate constants that are in good agreement with those determined by lifetime quenching. Thus, there is no emission observed from the protonated excited state. In addition, solutions of authentic $\text{ReO}(\text{OH})(\text{py})_4^{2+}$ can be

(20) Kalsbeck, W. A.; Thorp, H. H. *J. Am. Chem. Soc.* **1993**, *115*, 7146.

(21) Strouse, G. F.; Anderson, P. A.; Schoonover, J. R.; Meyer, T. J.; Keene, F. R. *Inorg. Chem.* **1992**, *31*, 3004.

(22) Kristjánssdóttir, S. S.; Norton, J. R. *J. Am. Chem. Soc.* **1991**, *113*, 4366.

(23) Wubbels, G. G. *Acc. Chem. Res.* **1983**, *16*, 285. Kresge, A. J. *Chem. Soc. Rev.* **1973**, *2*, 475. Albery, W. J. *Annu. Rev. Phys. Chem.* **1980**, *31*, 227.

(24) Yates, K. *J. Am. Chem. Soc.* **1986**, *108*, 6511. McEwen, J.; Yates, K. *J. Am. Chem. Soc.* **1987**, *109*, 5800.

(25) Yates, K. *J. Phys. Org. Chem.* **1989**, *2*, 300.

(26) Giordano, P. J.; Bock, C. R.; Wrighton, M. S.; Interrante, L. V.; Williams, R. F. X. *J. Am. Chem. Soc.* **1977**, *99*, 3187.

(27) Davila, J.; Bignozzi, C. A.; Scandola, F. *J. Phys. Chem.* **1989**, *93*, 1373.

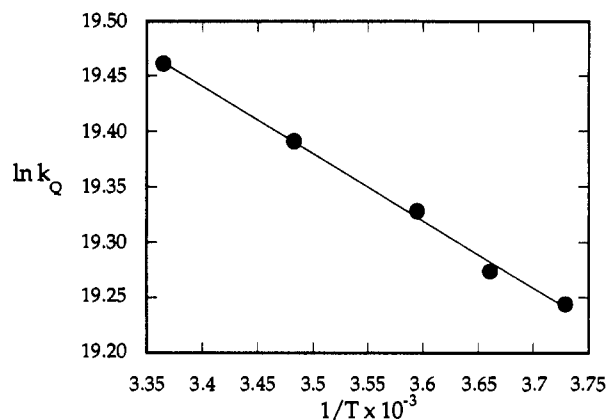
(28) Vining, W. J.; Neyhart, G. A.; Nielsen, S.; Sullivan, B. P. *Inorg. Chem.* **1993**, *32*, 4214.

(29) Sun, H.; Hoffman, M. Z. *J. Phys. Chem.* **1993**, *97*, 5014.

Table 2. Quenching Data for ReO_2^+ as a Function of Ancillary Ligands

quencher	$\text{p}K_a^a$ H_2O	$\text{p}K_a^b$ CH_3CN	$k_Q(\text{py})$, $\text{M}^{-1} \text{s}^{-1} c$	$k_Q(3\text{-Cl-py})$, $\text{M}^{-1} \text{s}^{-1} c$	$k_Q(4\text{-OMe-py})$, $\text{M}^{-1} \text{s}^{-1} c$
water (1)	15.7	30.0 ^d	9.5×10^5	4.0×10^5	1.8×10^7
1,4-dihydro-4-imino-1-methylpyrimidine hydroiodide (2)	12.2	19.7 ^e	3.5×10^7	3.6×10^7	1.9×10^7
triethylammonium hexafluorophosphate (3)	10.7	18.5	1.6×10^8	6.5×10^7	3.1×10^8
trimethylammonium tetraphenylborate (4)	9.8	17.6	3.4×10^8	7.9×10^7	5.4×10^8
ammonium hexafluorophosphate (5)	9.2	16.4	3.9×10^8	4.0×10^8	5.3×10^8
3-nitrophenol (6)	8.4	22.6	5.3×10^8	3.1×10^8	8.3×10^8
4-nitrophenol (7)	7.2	20.9	1.2×10^9	6.3×10^8	7.1×10^8
pyridinium <i>p</i> -toluenesulfonate (8)	5.2	12.3	9.5×10^8	9.6×10^8	9.6×10^8
benzoic acid (9)	4.2	20.7	1.3×10^9	1.3×10^9	9.0×10^8
4-nitrobenzoic acid (10)	3.4	18.7	8.8×10^8	1.0×10^9	1.1×10^9

^a Aqueous $\text{p}K_a$'s taken from ref 16. ^b Acetonitrile $\text{p}K_a$'s taken from ref 36. ^c Rate constants measured by Stern-Volmer emission intensity quenching in acetonitrile solution; error $\pm 10\%$. ^d $\text{p}K_a$ ' value from ref 41. ^e Obtained by extrapolation from the aqueous value; see text.

**Figure 2.** Temperature dependence of the rate constant for quenching of $[\text{ReO}_2(\text{py})_4](\text{PF}_6)$ (0.27–0.35 mM) by 2,6-di-*tert*-butylpyridinium.

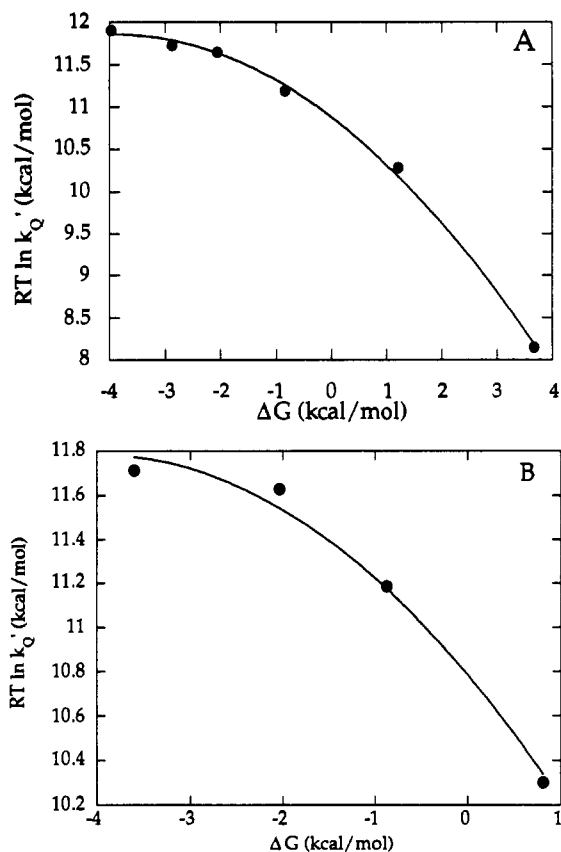
prepared in strong acid,³⁰ and these solutions show no emission. Hupp and co-workers have prepared $\text{ReO}(\text{OMe})_2^{2+}$ complexes that can be dissolved in nonaqueous solvents, and these complexes have identical absorption energies identical to those of $\text{ReO}(\text{OH})_2^{2+}$ complexes but also have no measurable excited-state lifetime or emission.^{31,32} Finally, the ligand-field absorption energy for $\text{ReO}(\text{OH})_2^{2+}$ is 4400 cm^{-1} lower than that for ReO_2^+ , so the energy-gap law, which has been shown to apply to this family of complexes,³³ predicts a much shorter lifetime for $\text{ReO}(\text{OH})_2^{2+}$.

The values of k_Q determined for the three metal complexes are given in Table 2. The calculated curvature ($d\alpha/d\Delta G$, eq 2) for the rate constants for $\text{ReO}_2(\text{py})_4^+$ is 0.13 kcal^{-1} , as determined by published procedures.²⁴ This gives a value for λ of 3.9 kcal and an intrinsic barrier of 0.98 kcal (points taken at $\text{p}K_a < 8$ were neglected because the diffusion-controlled limit clearly dictates the dynamics in this region). This low value of λ is consistent with estimates by Yates of barriers to excited-state proton-transfer reactions that proceed at diffusion-controlled rates. To verify this low barrier, the quenching rate constant for 2,6-di-*tert*-butylpyridinium was measured as a function of temperature. The slope of the plot of $\ln k_Q$ versus $1/T$ (Figure 2) gives a ΔG^\ddagger of 1.2 kcal/mol , which is similar to the barrier of 0.98 kcal calculated from the curvature of the free-energy dependence of K_Q .

With a good estimate for λ in hand, the data in Table 2 for $\text{ReO}_2(\text{py})_4^+$ could then be fitted to the Marcus equation in the form

$$RT \ln k_Q' = RT \ln k_Q'(0) - \Delta G/2 - \Delta G^2/4\lambda \quad (3)$$

where k_Q' is the measured rate constant corrected for diffusion,³⁴

**Figure 3.** (a) Free-energy dependence for quenching of $\text{ReO}_2(\text{py})_4^{2+}$ by the acids in Table 2. The free-energy axis was calculated from the aqueous $\text{p}K_a$'s of the quenchers and the $\text{p}K_a^*$ obtained from fitting to eq 3 (solid line) with λ held fixed at 3.9 kcal/mol . The fitted parameters are $k_Q'(0) = 9.5 \times 10^7 \text{ M}^{-1} \text{ s}^{-1}$ and $\text{p}K_a^* = 11.3$ (aqueous scale). (b) Free-energy dependence for quenching of $\text{ReO}_2(\text{py})_4^{2+}$ by quenchers 2–5. The free-energy axis was calculated from the acetonitrile $\text{p}K_a$'s of the quenchers and the $\text{p}K_a^*$ obtained from fitting to eq 3 (solid line). The fitted parameters are $k_Q'(0) = 8.1 \times 10^7 \text{ M}^{-1} \text{ s}^{-1}$ and $\text{p}K_a^* = 19.1$ (acetonitrile scale).

$k_Q'(0)$ is constant for a particular series of quenchers, and λ was held fixed at the determined value of 3.9 kcal . The two-parameter least-squares fit is shown in Figure 3 where the solid line was calculated using $k_Q'(0) = 9.5 \times 10^7 \text{ M}^{-1} \text{ s}^{-1}$ and $\text{p}K_a^* = 11.3$. This value for $k_Q'(0)$ is similar to others determined for electron-transfer reactions involving related excited states.^{34,35} Upon excitation, the $\text{p}K_a$ of $\text{Re}(\text{O})(\text{OH})_2^{2+}$ changes by over 11 units, which is consistent with values determined for other excited-

(30) Pipes, D. W.; Meyer, T. J. *Inorg. Chem.* **1986**, *25*, 3256.(31) Ram, M. S.; Jones, L. M.; Ward, H. J.; Wong, Y.-H.; Johnson, C. S.; Subramanian, P.; Hupp, J. T. *Inorg. Chem.* **1991**, *30*, 2928.

(32) Ram, M. S.; Skeens-Jones, L. M.; Johnson, C. S.; Zhang, X. L.; Hupp, J. R. Unpublished results.

(33) Brewer, J. C. Ph.D. Thesis, California Institute of Technology, 1991.

(34) Bock, C. R.; Connor, J. A.; Gutierrez, A. R.; Meyer, T. J.; Whitten, D. G.; Sullivan, B. P.; Nagle, J. K. *J. Am. Chem. Soc.* **1979**, *101*, 4815.(35) (a) Marshall, J. L.; Stobart, S. R.; Gray, H. B. *J. Am. Chem. Soc.* **1984**, *106*, 3027. (b) Nocera, D. G.; Gray, H. B. *J. Am. Chem. Soc.* **1981**, *103*, 7349.

state proton transfers²³⁻²⁹ and with the increase in oxygen basicity that can be predicted from the electronic structure of the excited state.⁹⁻¹⁵

Adequately describing the free-energy dependence of proton transfer to ReO_2^{+*} using eq 3 requires that the linear term be $\Delta G/2$, giving a value for α ($=d\Delta G^\ddagger/d\Delta G$) of 0.5 at $\Delta G = 0$. This implies that the ground- and excited-state potential energy surfaces look relatively similar (Figure 1). This probably results from the largely metal-based character of the $d_{xz,yz}$ orbitals. As a result, the difference between pK_a and pK_a^* is only 11 units as opposed to 15–20 units in organic systems.²³⁻²⁵

A concern in our analysis of the data in Table 2 is that the experiments are performed in acetonitrile, but the pK_a 's used in the analysis are for aqueous solution. The acetonitrile pK_a 's are given for comparison in Table 2 and, as we have pointed out earlier,¹⁶ do not give the same smooth trend with quenching rate constant as the aqueous pK_a 's. The cationic nitrogen acids (3–5 and 8) dissociate in acetonitrile in the same manner as in water,³⁶ so the behavior of these quenchers is analogous in both solvents. The quenchers are simply more basic in acetonitrile than water by approximately the same amount across the series. It is apparent from Table 2 that the acetonitrile pK_a 's for these quenchers are greater than the aqueous pK_a 's by 7.5 ± 0.36 units,³⁶ which is in agreement with the difference noted by Norton for related acids.³⁷ Since quencher 2 is also a cationic nitrogen acid, it is reasonable to assume that its pK_a will follow the same trend, which gives a value of 19.7, as indicated in Table 2. Quencher 8 is clearly in the diffusion-limited region, but this still provides four homologous quenchers (2–5) with pK_a 's known in acetonitrile that can be analyzed. Fitting of eq 3 (with $\lambda = 4$ kcal/mol) to the rate constants for these four quenchers gives the results shown in Figure 3B. The fitting provides a value of $k_Q'(0) = 8.1 \times 10^7 \text{ M}^{-1} \text{ s}^{-1}$, which is in very good agreement with that obtained by fitting the entire series of quenchers using the aqueous pK_a 's (Figure 3A). More important, the pK_a^* obtained from Figure 3B is 19.1 on the acetonitrile scale. This value is equivalent to a pK_a^* on the aqueous scale of 11.6, which is in good agreement with that determined from Figure 3A with the entire series of quenchers. Allowing λ to float does not change the results significantly.

Our earlier work on metal hydride complexes¹⁷ will also allow us to relate the analysis in Figure 3 to an analysis based on a family of quenchers with pK_a 's that are known in acetonitrile solution. We have shown that metal hydride complexes quench the emission of $\text{ReO}_2(\text{py})_4^{+*}$ efficiently and that the rate constants for quenching can be described using eq 4,¹⁷ where k_{11} and k_{22}

$$k_Q = (k_{11}k_{22}K_{\text{eq}})^{1/2} \quad (4)$$

are the self-exchange rate constants for the metal hydride complex and the $\text{ReO}_2(\text{py})_4^{+*}$ excited state, respectively, and K_{eq} is the equilibrium constant for the reaction. These quenchers have very large intrinsic barriers to proton transfer,^{22,38,39} so eq 4 is appropriate for analyzing the free-energy dependence of the k_{11} 's are known. In our earlier work,¹⁷ we were able only to calculate ratios of k_Q 's for different quenchers, because the values of k_{22} for $\text{ReO}(\text{OH})^{2+*}$ and the pK_a^* are not known. The results from the metal hydride quenchers, whose thermodynamic and kinetic acidities are well determined in acetonitrile, can be related to the results on oxygen and nitrogen acids discussed here via the parameter $k_Q'(0)$ obtained from fitting in Figure 3.

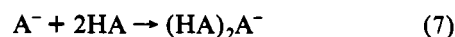
The $k_Q'(0)$ parameter represents the quenching rate constant at $\Delta G = 0$, which, from substitution of $K_{\text{eq}} = 1$ into eq 4, gives³⁴

$$k_Q'(0) = (k_{11}k_{22})^{1/2} \quad (5)$$

A requirement for using eq 3 to analyze rate constants for a series of quenchers is that the quenchers must all have similar k_{11} 's. The quenchers used here all under diffusion-controlled proton transfer,³⁷ and we have shown previously that rate constants for carbon acids and metal hydrides, which have appreciable barriers to proton transfer, do not fit on the curve defined by the points in Figure 3.¹⁷ Thus, we can estimate that $k_{11} = 10^9 \text{ M}^{-1} \text{ s}^{-1}$ for the series of quenchers in Figure 3. From the $k_Q'(0)$ determined from fitting to eq 3, we can then estimate that $k_{22} = 10^7 \text{ M}^{-1} \text{ s}^{-1}$ for the self-exchange reaction of $\text{ReO}(\text{OH})^{2+}$. A rate constant for self-exchange for the rhenium complex that is somewhat lower than the diffusion-controlled limit can be attributed to electronic reorganization due to the change in multiple-bonding character in the ReO_2^+ unit upon protonation.

From an estimate of $k_{22} = 10^7 \text{ M}^{-1} \text{ s}^{-1}$, the rate constants for quenching by metal hydride complexes can be used to estimate pK_a^* using eq 4. This procedure will allow us to relate the rate constants determined here to those of the metal hydride quenchers, where complete thermodynamic and kinetic acidity data in acetonitrile are available and where we have shown that eq 4 is operative.¹⁷ Using the metal hydride rate constants, we estimate a pK_a^* (on the acetonitrile scale) of 19.6. This value is equivalent to a pK_a^* on the aqueous scale of 12.1,³⁷ which is in reasonably good agreement with the values of 11.3 and 11.6 determined from fitting the data in Figure 3 to eq 3. Norton has suggested an error in correlating aqueous and acetonitrile pK_a 's of ± 1 unit,³⁷ and the range of pK_a values determined by the three different methods described here (11.3–12.1) is consistent with this estimate. The good agreement between determined pK_a values suggests that Marcus theory is operative both in the large-barrier metal hydride case¹⁷ and in the small-barrier case discussed here, providing the appropriate equation is used to analyze the data.

The analysis of the complete set of quenching data as a function of the aqueous pK_a apparently gives a valid estimate of the pK_a^* in acetonitrile, since separate determination using the acetonitrile pK_a 's in Figure 3B gives the same result. The calculation of the same pK_a from the metal hydride quenchers further supports the validity of the analysis. The important question then is, Why do the aqueous pK_a 's of the phenols and benzoic acids accurately predict the quenching rate constant when the acetonitrile pK_a 's do not? The acetonitrile pK_a 's of the phenols and benzoic acids do not fall in the trend defined by the cationic nitrogen acids because these neutral acids do not behave the same way in acetonitrile and water. In acetonitrile, these acids undergo extensive homoconjugation (eq 6) and often exist as dimeric species (eq 7).⁴⁰ As a result, these acids appear considerably more basic



than cationic nitrogen acids of similar aqueous pK_a . A somewhat better correlation between the quenching rate constants and thermodynamic acidity data for acetonitrile is obtained when pK_a' values are used. The value of pK_a' is derived from the pK_a after correlation for the activity of the proton in the particular solvent used for the measurement.⁴¹ Nonetheless, the pK_a' values for acetonitrile still do not fall in the same order as the quenching rate constants.

(36) Coetzee, J. F. *Prog. Phys. Org. Chem.* **1967**, *4*, 45. We are grateful to a reviewer for pointing this out.

(37) Kristjánssdóttir, S. S.; Norton, J. R. *Transition Metal Hydrides*; Dedieu, A., Ed.; VCH Publishers: New York, 1992; p 309.

(38) Kristjánssdóttir, S. S.; Norton, J. R.; Moroz, A.; Sweany, R. L.; Whittenburg, S. L. *Organometallics* **1991**, *10*, 2357.

(39) Eddin, R. T.; Sullivan, J. M.; Norton, J. R. *J. Am. Chem. Soc.* **1987**, *109*, 3945. Moore, F. J.; Sullivan, J. M.; Norton, J. R. *J. Am. Chem. Soc.* **1986**, *108*, 2257.

(40) Coetzee, J. F.; Padmanabhan, G. R. *J. Phys. Chem.* **1965**, *69*, 3193.

(41) Barrette, W. C., Jr.; Johnson, H. W., Jr.; Sawyer, D. T. *Anal. Chem.* **1984**, *56*, 1890.

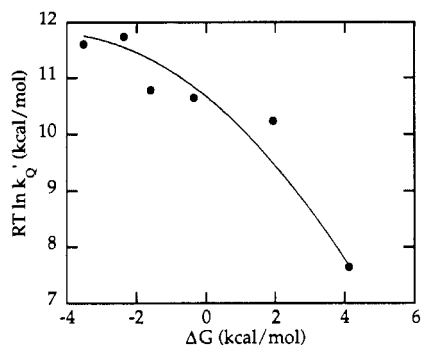


Figure 4. Free-energy dependence for quenching of $\text{ReO}_2(3\text{-Cl-py})_4^{+*}$ by the acids in Table 2. The free-energy axis was calculated from the aqueous $\text{p}K_a$'s of the quenchers and the $\text{p}K_a^*$ obtained from fitting to eq 3 (solid line).

We have suggested previously that the dependence of the quenching rate constant on the aqueous $\text{p}K_a$ may result from the mediation of the proton transfer by a hydrogen-bonded intermediate.¹⁶ Within this hydrogen-bonded intermediate, the aqueous $\text{p}K_a$ may be the best measure of the thermodynamics of proton transfer. Since making this suggestion, we have demonstrated that hydrogen bonding does indeed accelerate the reaction.¹⁷ This results in Table 2 can be understood if the species AHA^- and $(\text{HA})_2\text{A}^-$ also quench $\text{ReO}_2(\text{py})_4^{+*}$ efficiently. While somewhat hindered sterically, formation of hydrogen bonds between these species and $\text{ReO}_2(\text{py})_4^{+*}$ will be encouraged by electrostatic interaction so that dimerization and homoconjugation may not affect the ability of the acid to quench the excited state. These observations present the idea that $\text{ReO}_2(\text{py})_4^{+*}$ quenching may ultimately be used to quantitate conveniently the intrinsic acidity of a given quencher in a nonaqueous solvent without complications arising from homoconjugation or dimerization.

Since we have shown that fitting the complete set of data as a function of aqueous $\text{p}K_a$ gives the same results as fitting the data for the cationic nitrogen acids as a function of acetonitrile $\text{p}K_a$, we will fit the complete set of data for the other two complexes discussed here. Fitting of the free-energy dependence for quenching rate constants of $\text{ReO}_2(4\text{-OMe-py})_4^{+*}$ and $\text{ReO}_2(3\text{-Cl-py})_4^{+*}$ has also been undertaken. For the 3-Cl-py derivative, analysis using the standard Marcus relation is straightforward (Figure 4), giving a value for λ of 4.2 kcal, which is similar to that obtained for $\text{ReO}_2(\text{py})_4^{+*}$. The determined $\text{p}K_a^*$ for $\text{ReO}(\text{OH})(3\text{-Cl-py})_4^{2+}$ is 11.0, which is lower than the $\text{p}K_a^*$ of $\text{ReO}(\text{OH})(\text{py})_4^{2+}$ by approximately the same amount as the difference in ground-state $\text{p}K_a$'s (Table 1).

The 4-OMe-py complex, however, does not yield to straightforward analysis. Fitting to eq 3 is not satisfactory, apparently because the linear $\Delta G/2$ term cannot be accommodated by the data. Instead, the analysis of Yates^{24,25} was undertaken, using the equation

$$\Delta G^\ddagger = RT \ln k_Q'(0) - \epsilon \Delta G/2 - \epsilon^2 (\Delta G)^2 / 4\lambda \quad (8)$$

where ϵ is a parameter related to the degree of distortion in the excited state relative to the ground state. The value of ϵ must be between 0 and 1, with $\epsilon = 1$ in the limit of no excited-state distortion. Thus, when $\epsilon = 1$, eq 8 reduces to the standard Marcus relation. It has been shown that $\epsilon = m/n$ where m is the force constant of a pertinent excited-state vibrational frequency and n is the force constant of the ground-state frequency for the same vibrational mode.²⁵

Analysis of the rate data for $\text{ReO}_2(4\text{-OMe-py})_4^{+*}$ using eq 8 was performed by first setting λ at 4 kcal on the basis of the fits for $\text{ReO}_2(\text{py})_4^{+*}$ and $\text{ReO}_2(3\text{-Cl-py})_4^{+*}$. Fitting then yielded a value for ϵ of 0.7 and a $\text{p}K_a^*$ for $\text{ReO}(\text{OH})(4\text{-OMe-py})_4^{2+*}$ of 12.0 (Figure 5). The data could also be subjected to a three-parameter fit by allowing ϵ to float along with $\text{p}K_a^*$ and λ . This fit gives slightly higher values for all three parameters, with $\epsilon =$

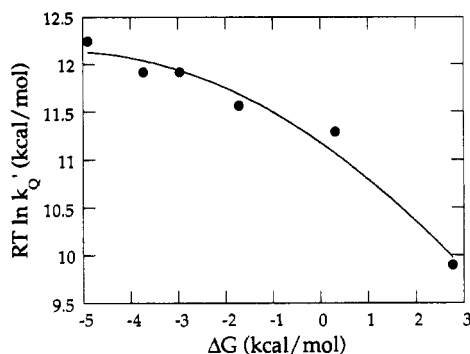


Figure 5. Free-energy dependence for quenching of $\text{ReO}_2(4\text{-OMe-py})_4^{+*}$ by the acids in Table 2. The free-energy axis was calculated from the aqueous $\text{p}K_a$'s of the quenchers and the $\text{p}K_a^*$ obtained from fitting to eq 8 (solid line).

Table 3. Vibrational Frequencies (cm^{-1}) as a Function of Ancillary Ligands

complex	ν^- ($\text{Re-O}_{\text{asym}}$) ^a	ν^- (Re-O_{sym}) ^b	ν^- ($\text{Re-O}_{\text{sym}}^*$) ^c	ϵ^- (meas) ^d
$\text{ReO}_2(3\text{-Cl-py})_4^{+*}$	814	900	740	0.7
$\text{ReO}_2(\text{py})_4^{+*}$	816	907	744	0.7
$\text{ReO}_2(4\text{-OMe-py})_4^{+*}$	810	902	709	0.6

^a From IR spectra.^{31,33} ^b From resonance Raman spectra. ^c From 77 K absorption spectra. ^d $\epsilon = [\nu(\text{Re-O}_{\text{sym}}^*)/\nu(\text{Re-O}_{\text{sym}})]^2$.

0.78, $\lambda = 4.8$ kcal, and $\text{p}K_a^* = 12.5$. As seen in Table 1, the values for the $\text{p}K_a^*$'s closely track the ground-state $\text{p}K_a$'s, providing support for the validity of the chosen model. The need for the ϵ parameter suggests that greater excited-state distortion exists in $\text{ReO}_2(4\text{-OMe-py})_4^{+*}$ than in the other derivatives. This may be understood in terms of the electron-releasing character of the 4-OMe-py ligand. A more electron-rich rhenium center may result in more covalent Re-O bonds, which would in turn lead to greater excited-state distortion.

The parameter ϵ is associated with the degree of excited-state distortion in the functionality participating in proton transfer.²⁵ As stated above, the parameter is equivalent to m/n where m is the force constant of an excited-state vibrational frequency and n is the force constant of the analogous ground-state frequency. The vibrational mode chosen to calculate ϵ must be strongly coupled to the proton-transfer reaction, and the clear choice in our case is the Re-O stretch. The asymmetric Re-O stretch, obtained from IR spectra, does not change appreciably upon substitution of the pyridine rings (Table 3). The symmetric Re-O stretch was measured by Hupp et al. for the pyridine complex by resonance Raman spectroscopy.⁴² As expected, the Re-O mode is strongly coupled to the low-energy ligand field ($d_{xy}^2 \rightarrow d_{xy}^1 d_{xz}^1 d_{yz}^1$) transition, as seen in low-temperature emission spectra.⁹ We have measured the analogous frequencies for the 3-Cl-py and 4-OMe-py complexes, and the spectrum of $\text{ReO}_2(4\text{-OMe-py})_4^{+*}$ is shown in Figure 6. The frequencies for the symmetric Re-O stretch in all three complexes are given in Table 3.

Low-temperature absorption spectra of the ligand-field band in ReO_2^{+} complexes show a vibrational progression in the excited-state, symmetric Re-O stretch.⁹ We have obtained spectra of the pyridine, 3-Cl-py, and 4-OMe-py complexes at 77 K. The spectrum of the 4-OMe-py complex is shown in Figure 7. The frequency determined from our spectrum of the pyridine complex is in good agreement with that determined by Winkler and Gray.⁹ The values for the three complexes are shown in Table 3. The frequencies for the py and 3-Cl-py complexes are similar, but the frequencies for the 4-OMe-py complex is significantly lower.

Measured values of ϵ can be calculated from the vibrational frequencies for the ground- and excited-state Re-O symmetric

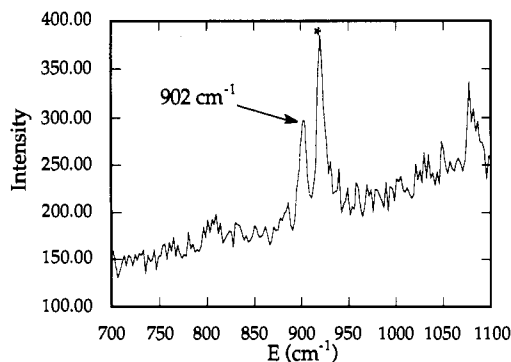


Figure 6. Resonance Raman spectrum of $[\text{ReO}_2(4\text{-OMe-py})_4](\text{PF}_6)$ (5.4 mM) showing the symmetric Re–O stretch at 902 cm^{-1} . The band indicated with an asterisk is due to the acetonitrile solvent.

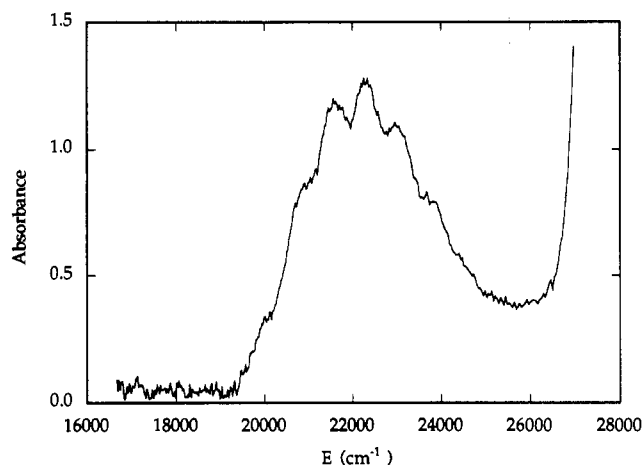


Figure 7. Absorption spectrum of $\text{ReO}_2(4\text{-OMe-py})_4^+$ (0.62 mM) at 77 K in a 2:1 2-methyltetrahydrofuran/methanol glass slowing the vibrational progression due to the excited-state symmetric Re–O stretch.

stretch. These ϵ values are shown in Table 3. The 4-OMe-py complex does have a measurably lower value of ϵ , which supports our use of eq 8 in analyzing the rate constants. In addition, the measured magnitude of ϵ is in reasonably good agreement with the values obtained from fitting (Table 1). Nevertheless, the difference in ϵ for the 4-OMe-py complex compared to the py and 3-Cl-py complexes is relatively small. Apparently, the fitting procedure is not sensitive enough to require the ϵ parameter in the other two cases, probably because the absolute magnitudes

of the excited-state distortions are too small (i.e., ϵ is close to 1). Fitting of data from organic systems where eq 8 is used requires ϵ values of 0.33–0.5 in order to make reasonable estimates of λ .^{24,25} Clearly, these large distortions in covalent systems show much larger effects of inclusion of the ϵ parameter, making determinations from fitting much easier.

The model used thus far in describing the free-energy dependence of the proton-transfer kinetics is satisfying in a number of ways. Values for $\text{p}K_a$'s are obtained that quantitatively track the ground-state $\text{p}K_a$'s across the three ReO_2^+ derivatives. The calculated intrinsic barriers ($\lambda \sim 4$ kcal) are in good agreement with those estimated by others for proton transfers that occur with such rapid kinetics.^{24,25} Temperature-dependent quenching experiments support these small barriers (Figure 2). The value of $k_Q'(0)$ is in good agreement with those determined in electron-transfer cases where self-exchange for both partners is rapid³⁴ and can be used to relate rate constants for quenching by acids with small barriers to protonation to those for acids with relatively large barriers.^{16,17} Using this $k_Q'(0)$ parameter, similar values of $\text{p}K_a^*$ can be estimated from both families of quenchers.

The ability to use the unaltered eq 3 in the analyses of the proton-transfer dynamics of $\text{ReO}_2(\text{py})_4^+$ and $\text{ReO}_2(3\text{-Cl-py})_4^+$ is consistent with the largely ionic character of the Re–O bonds in these complexes; however, addition of electron-releasing substituents such as OMe to the complex renders the rhenium center more electron-rich and increases the covalency, and hence the π^* character, of the excited-state. This creates a need for the ϵ parameter in analyzing the proton-transfer dynamics of $\text{ReO}_2(4\text{-OMe-py})_4^+$. Measured ground- and excited-state vibrational frequencies are qualitatively consistent with the need for ϵ in analyzing the rate constants for the 4-OMe-py complex. This points out that the dynamics of proton transfer can be profoundly affected by the electronic structure of the metal complex. Thus, the electronic structure of the metal complex can influence both the intrinsic barrier, in the form of λ , and the position of the transition state along the reaction coordinate, in the form of ϵ .

Acknowledgment. We thank Dr. R. J. Kessler for assistance with the Raman measurements, and we thank the donors of the Petroleum Research Fund, administered by the American Chemical Society, for support of this research. H.H.T. is a Presidential Young Investigator and a Fellow of the David and Lucile Packard Foundation. The Raman spectrophotometer was purchased with funds from the NIH (Grant 1-S10-RR04089-01).